Chemistry SELECT

www.chemistryselect.org

A journal of ChemPubSoc Europe

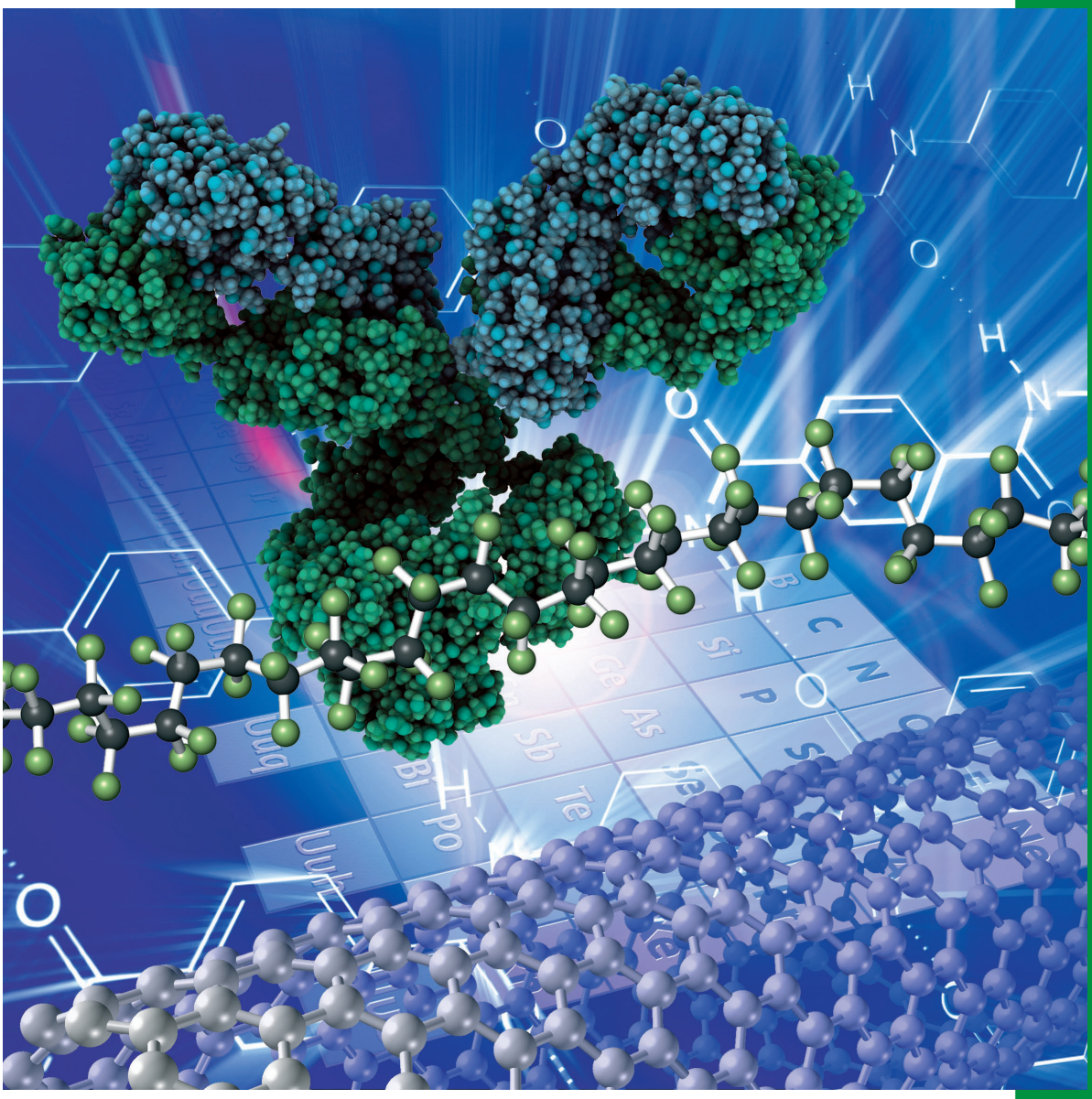

REPRINT

WILEY-VCH

ChemPubSoc Europe

DOI: 10.1002/slct.201803295

Chemistry SELECT Full Papers

Catalysis

Environmentally Benign Approach for the Synthesis of Azo Dyes in the Presence of Mesoporous Sulfated Core-Shell Zirconia-Copper(I) Oxide Solid Acid Catalyst

Lakshminarayana Parashuram,[a, b] Swamy Sreenivasa,*[a] Sathyanarayana Rao Akshatha,[a] Velu Udaya Kumar,[c] and Sandeep Kumar[d]

Sulfated solid acid catalyst finds application mainly in the reactions which requires acid sites. Synthesis of azo dyes by diazo coupling in presence of sulfated core shell zirconia-copper oxide solid acid catalyst (Cu(I)@ZrO_2-SO_4^{2-}) has been discussed hereunder. A detailed investigation on, the effect of sulfate loading, surface area and surface acidity for the synthesis of azo dyes has been demonstrated. As sulfate loading increased on the catalyst, it decreased its surface area and this was evident from the Brunauer Emmett Teller surface area analysis. The robust catalytic activity of Cu(I)@ZrO_2-SO_4^{2-} catalyst was due to its super acidity, which arises due to the presence of both Bronsted and Lewis acid sites, this was experimentally confirmed by Pyridine-Fourier transform infrared spectroscopy and ammonia-temperature programmed desorption studies. X-ray diffraction, transmission electron microscopy and selected area electron diffraction techniques provided detailed information about the effect of sulfate loading on phase and crystal structure of the catalyst. In the present work we describe a simple, efficient and environmentally benign catalytic process for the synthesis of azo dyes.

Introduction

Solid acid heterogeneous transition metal oxide catalysts are widely explored in industrial and environmental processes due to their constructive impacts. Due to the environmental concern, it is the deciphering knowledge a synthetic chemist must have to design environmentally benign catalytic technologies. In this path, solid acid catalysts find very extensive applications in chemical and refinery industries. There are constant efforts by the synthetic chemists to replace hazardous, polluting inorganic acid catalysts by solid acid catalysts.[1] A number of organic transformations have been performed using solid acid catalysts, for better selectivity and yields than conventional catalysis.[2–5] Presence of both Bronsted and Lewis acidity in supported solid acids significantly contributes to the enhanced activity.[6,7]

Zirconia is stable metal oxide support due to its high dielectric constant,[8] chemical and thermal stability[9,10] and exhibits amphoteric nature.[11] The Bronsted-Lewis acidity of zirconia can be significantly enhanced by sulfate loading on it, which results in a super acid.[12] Out of the many super acids explored, sulfated zirconia is a material of interest for most catalysis researchers. This is due to the fact that sulfated zirconia is a robust catalytic material due to its high surface area,[13] high surface super acidity competent than inorganic acids[14,15] and also it offers facile recoverability and reusability.

Experimental conditions and preparation methods significantly influence the catalytic properties of sulfated zirconia. Since, the catalyst preparation protocol like mode of precipitation, calcination temperature and method of sulfate loading will significantly influence surface area and surface acidity and these effects in turn influence its catalytic performance.[16] Hence, there is significant role of a synthetic chemist to design a tailor made solid acid for desired transformation.

There are reports which have discussed the effect of presence of other transition metal ions on the catalytic performance of the sulfated zirconia. These transition metal ions incorporated to sulfated zirconia can lead to more active solid acid catalysts. J. Liu et. al. reported selective isomerization of α-pinene over iron doped sulfated zirconia catalyst.[17,18] In this context, zirconia lattice containing +1 oxidation state stabilized copper ions serves as a very good redox catalyst. Its catalytic activity for the synthesis of quinazolinones has been discussed in detail in our previous report elsewhere.[19]

Many reports which successfully addressed the activity and selectivity issues in chemical transformation using of solid acid catalysts are available.[20–24] There are many precursors to load the acid sulfate ions on to the metal oxide support, out of which sulfuric acid and ammonium sulfate are the two most explored precursors. In the present work, we have used aqueous sulfuric acid as the direct source of sulfate ions, the

[a] L. Parashuram, Dr. S. Sreenivasa, S. R. Akshatha
Department of Studies and Research in Organic Chemistry, Tumkur University, Tumkur-572101, (India)
Tel.: +919620230672
E-mail: drsreenivasa@yahoo.co.in
[b] L. Parashuram
New Horizon College of Engineering, (affiliated to VTU Belagavi), Kadubeesanahalli, Bangalore- 560103, (India)
[c] Dr. V. U. Kumar
Department of Chemistry, Siddaganga Institute of Technology, (affiliated to VTU Belagavi), B.H. Road, Tumkur-572103, (India)
[d] S. Kumar
Raman Research Institute, C.V. Raman Avenue, Bangalore-560080, (India)

Supporting information for this article is available on the WWW under https://doi.org/10.1002/slct.201803295

sulfate loaded catalyst was further stabilized by subsequent calcination.

It is a field of ever interest for a synthetic chemist to explore the color chemistry. Because of exciting opportunities and advancement of these dyes in the field of sensors to promote the electro-catalytic activity,[25,26] photo material in optical storage applications,[27,28] as diagnosis probes in medical applications[29] and electronic devices.[30] Azo dyes also find applications in the field of dye sensitized electrodes for water splitting reaction,[31] coloring the textile fibers and as important intermediates in organic synthesis.[32] However, there is great concern and focus for the environmentally benign protocol, as many reports fails to address the problems like unsatisfactory yield, tedious reaction steps and longer reaction time. Therefore, designing a chemical protocol having less impact on environment, higher activity and selectivity is still a challenge in case of diazotization-coupling reaction.

Recently, Jinjing Qiu *et al.*[33] reported 1, 5-naptalenesulfonic acid stabilized diazonium salts of aromatic amines as stable source for diazotization and coupling reaction with various coupling agents. Mechanistic studies reveal that, 1, 5-naptalenesulfonic acid in presence of *tert*-butyl nitrite gave stable diazonium salts, these salts on addition of suitable coupling agent produced corresponding azo dye. Also Hassan Valizadeh et. al,[34] Alireza Najafi Chermahini et. al,[35] Amin Zarei et. al,[36] have reported carboxyl and nitrite functionalized graphene, modified clays and silica sulfuric acid as solid acid materials for diazotization reaction for the synthesis of azo dyes under environmentally benign protocol. In complimentary to these studies, the current investigation aims to demonstrate the effectiveness of *Cu(I)@ZrO$_2$-SO$_4^{2-}$* solid acid catalyst for the catalytic synthesis of azo dye under grinding, solvent free conditions. *Cu(I)@ZrO$_2$-SO$_4^{2-}$* catalyst was prepared by simple co-precipitation method, followed by sulfation using sulfuric acid and further stabilized by calcination at desired temperature.

BET surface analysis and NH_3-TPD methods were used to correlate the effect of sulfate loading on the catalytic activity ofThe neat FTIR spectrum of thin wafers *Cu(I)@ZrO$_2$-SO$_4^{2-}$*. The solid acid was successfully utilized to construct an environmentally benign protocol for the synthesis of azo dyes at room temperature following simple grinding method under solvent free conditions.

Results and Discussion

Structural study of preapared Cu(I)@ZrO$_2$-SO$_4^{2-}$ catalyst:

To ascertain the phases and crystal structure Cu(I)@ZrO$_2$-SO$_4^{2-}$ (5-20% sulfate loading) samples were analyzed by X-ray diffraction using Panalytical X-ray diffractometer. From the XRD spectrum shown in (Figure 1), it is evident that the peaks due to ZrO_2 are dominant in all cases. No significant peaks due to copper were detected in any of the material; hence a detailed analysis of dopant copper was not carried out.

The pure ZrO_2:Cu(I) showed cubic phase which is in good match with the crystal data with PDF card number 27–997. On

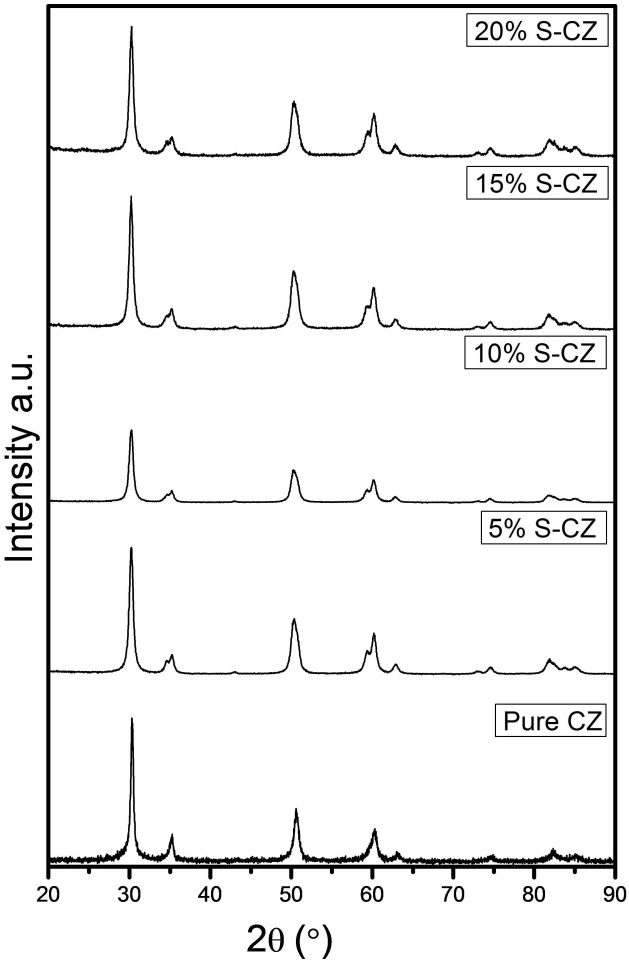

Figure 1. XRD spectrum of ZrO_2-Cu(I) and Cu(I)@ZrO_2-SO_4^{2-} (5-20%)

5% sulfate loading, ZrO_2:Cu(I) catalyst transformed from cubic phase to tetragonal phase with 2θ values positioned at 30.19, 34.66, 35.26, 50.35, 59.42, 60.23 and 62.91. Further, increase in sulfate loading resulted in increased peak intensity, however it didn't affect the crystal phase of ZrO_2:Cu(I). Moreover, sulfate loading didn't affect the crystallite size in any case. The average crystallite size as calculated by Scherrer equation was 15 nm.

Scherrer equation,

D is the average crystallite size, k is the shape factor = 0.94, λ = wavelength of X-ray (0.154056 nm); β is the full width at half maximum (FWHM), θ is the Bragg angle (in degrees).

FTIR and Pyridine-FTIR Characterization of Cu(I)@ZrO$_2$-SO$_4^{2-}$ Material

The neat FTIR spectrum of thin wafers of Cu(I)@ZrO$_2$-SO$_4^{2-}$ (5 and 10%) catalyst were recorded and shown in (Figure 2). Neat FTIR spectra of the catalyst showed intense band near

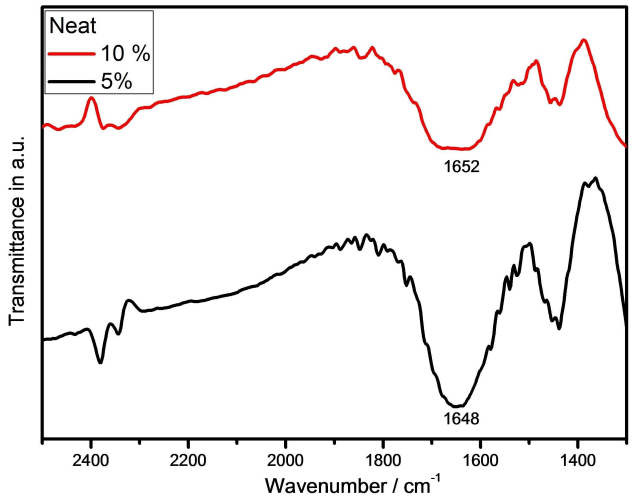

Figure 2. FTIR neat spectrum of Cu(I)@ZrO_2-SO_4^{2-} (5 and 10%)

1650 cm^{-1} indicating strong affinity of sulfated catalyst towards water molecules.[37,38]

To record the pyridine-FTIR – thin wafers of Cu(I)@ZrO_2-SO_4^{2-} were developed by pelletizing them in a pellet press instrument. Then, these thin wafers were saturated with 5 µl of pyridine and heated in a hot air oven maintained at 120°C to remove physisorbed pyridine. Thus obtained wafers are cooled to room temperature and Pyridine-FTIR was recorded as shown in (Figure 3).[39] Further, to distinguish the nature of acidic sites

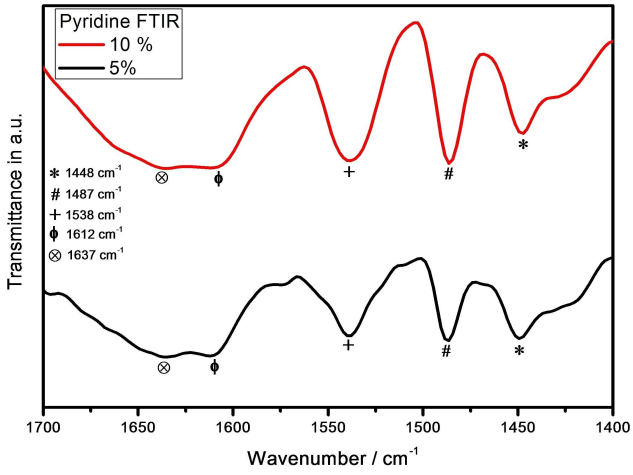

Figure 3. Pyridine FTIR spectrum of Cu(I)@ZrO_2-SO_4^{2-} (5 and 10%)

Bronsted/Lewis acidity (B/L) method was used. Relative ratio B/L was calculated from the peaks resulting from pyridine adsorbed to H^+ and Lewis acidic sites (1538 cm^{-1} and 1448 cm^{-1}). The B/L ratio of 5% and 10% sulfate loaded catalyst was almost closly same with values 0.86 and 0.88 respectively. Bronsted and Lewis acidity of Cu(I)@ZrO_2-SO_4^{2-} was arising due to the surface Zr-OH groups and surface sulfate groups respectively.

Thermo Gravimetric Analysis of Cu(I)@ZrO_2-SO_4^{2-} (5-20%)

To know the thermal stability of the loaded sulfate groups, Cu(I)@ZrO_2-SO_4^{2-} (5-20%) was subjected to thermo gravimetric analysis. Material with different sulfate loading showed weight loss in two steps, whereas 5% sulfate loaded Cu(I)@ZrO_2-SO_4^{2-} catalyst surprisingly showed weight gain of 3.9% as shown in (Figure 4). This tendency may be attributed to the oxidation of

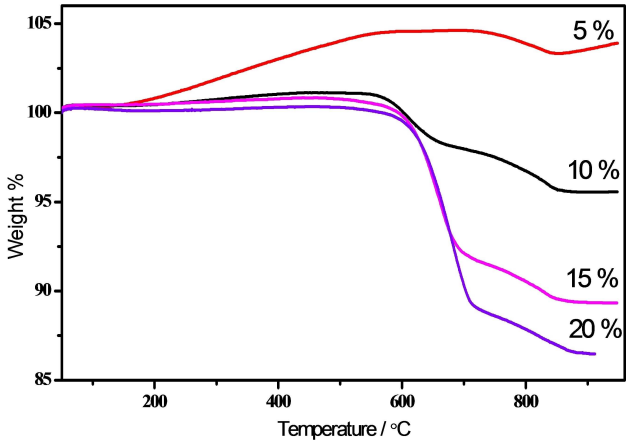

Figure 4. Thermo gravimetric analysis of Cu(I)@ZrO_2-SO_4^{2-} (5-20%)

copper(I)oxide to copper(II)oxide and a similar trend in the thermogravimetric analysis was reported by D. Farcasiu et. al.[40] Presence of sulfate groups on the surface would have facilitated the oxidation more significantly.

Further, in case of Cu(I)@ZrO_2-SO_4^{2-} with 10, 15 and 20% sulfate loading there is significant weight loss and no weight gain was observed. This may be due to the fact that, high sulfate loading would have damaged the core-shell structure of Cu(I)@ZrO_2-SO_4^{2-}, thereby resulting in oxidation of copper(I) oxide during initial calcination process itself.

The catalyst with 10, 15 and 20% of sulfate loading showed a total percentage weight loss of 5.57, 11.23 and 13.84 respectively. First step weight loss is between 550 to 700°C with percentage weight loss of 2.92, 8.31 and 10.78 respectively. The second step weight loss is between 700–870°C with percentage weight loss of 2.66, 2.92 and 3.07 respectively. The first step weight loss is attributed to the dehydroxylation of Cu(I)@ZrO_2-SO_4^{2-}[41] and the second step weight loss is attributed to the removal of bound sulfate groups.[42]

NH_3-Temperature Programmed Desorption

The amounts of acidity in mesoporous Cu(I)@ZrO_2-SO_4^{2-} (5-20%) catalysts were analyzed by temperature programmed desorption method. Ammonia is used as a probe molecule and the instrument is equipped with thermal conductivity detector.

Before performing ammonia desorption experiments, the sample was subjected to heat treatment at the desired temperature for an hour in helium atmosphere and then cooled to room temperature. Under maintained constant temperature, the sample was saturated with 10% ammonia in helium flow for 0.5 hours. The physisorbed ammonia probe molecules were removed by flushing the helium gas for an hour. After these pretreatment steps, desorption experiment was carried out in the temperature range of 100–600°C.

It is clearly evident from the TPD data that, 5% sulfate loaded Cu(I)@ZrO_2-SO_4^{2-} showed broad and intense signal. Further this broad peak was analyzed in detail using origin software, shown in (Figure 5). From the figure it is found that,

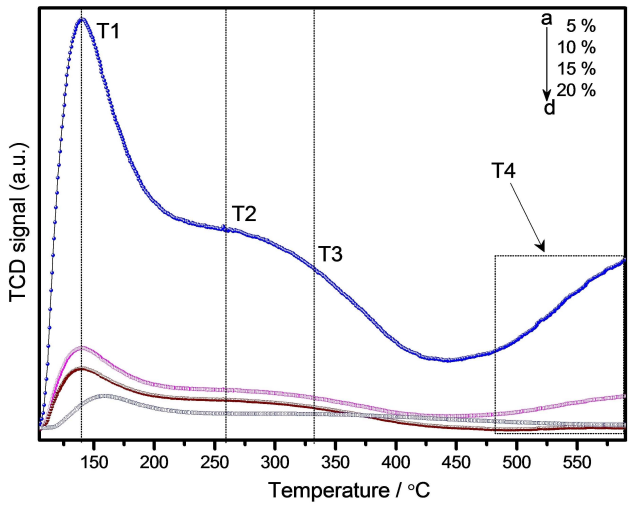

Figure 5. Ammonia temperature programmed desorption profiles of Cu(I)@ZrO_2-SO_4^{2-} (5-20%)

the signals at 145 °C, 260 °C, 330 °C and 500 °C are significant. The desorption value at T1 = 145°C is attributed to the weakly adsorbed ammonia to the surface terminal of ZrO_2:Cu(I) catalyst. The desorption at temperature T3 = 330°C will be due to the Bronsted acid sites i.e. arising due to -OH groups associated as Zr(Cu)-OH and the desorption at T2 around 260 °C is attributed to the Lewis acid sites.

The intensity of T2 and T3 peaks significantly reduced for 10, 15 and 20% sulfate loaded catalyst. This trend may be due to the fact that, higher quantity of sulfuric acid used would have damaged the core-shell structure, thereby facilitating direct conversion of copper from +1 to +2 oxidation state during catalyst preparation process itself. This facilitates the distribution of copper ions over the surface of the material, which significantly replaces the surface hydrogen ions, thereby decreasing the Bronsted acidity. Moreover a significant extra hump after 500 °C for 5% sulfate loaded catalyst has been observed, this is attributed to the strong Bronsted acid sites arising due to the induced normal Bronsted acid sites inside the cavities.

The intensity of the TCD signals decreased with increase in sulfate loading. The percentage intensities of TCD signals decrease in the order 20.45%, 15.45% and 8.6% compared to that of 5% sulfate loaded Cu(I)@ZrO_2-SO_4^{2-}. The B/L ratio calculated from the area of the peaks follow the order 0.653, 0.505, 0.373 and 0.391 respectively for 5–20% Cu(I)@ZrO_2-SO_4^{2-}.[43,44]

SEM and EDX of Cu(I)@ZrO_2-SO_4^{2-} (5-20%) catalyst

The morphology of Cu(I)@ZrO_2-SO_4^{2-} (5-20%) catalysts were determined by FESEM analysis, the micrographs are shown in the (Figure 6). All the mesoporous Cu(I)@ZrO_2-SO_4^{2-} catalysts showed uniform spherical morphology. It is evident from the analysis that sulfate loading didn't affect the particle size. However, the particles showed greater agglomeration with increase in sulfate loading, thereby decreasing the effective surface area. This trend clearly indicates incorporation of sulfate ions on surface.

The retention in the particle size and morphology may be attributed to the similar experimental procedure followed for the preparation of 5–20% sulfate loaded Cu(I)@ZrO_2-SO_4^{2-} catalyst. Further, EDX was recorded to evaluate the elemental composition and extent of sulfate loading as shown in (Figure 6). The graphs clearly indicate the presence of the elements Cu, Zr, O and S. The detailed elemental composition of Cu(I)@ZrO_2-SO_4^{2-} (5-20%) catalyst was presented as an inset in the EDX graphs.

TEM and SAED analysis of ZrO_2:Cu(I) and Cu(I)@ZrO_2-SO_4^{2-} catalyst

TEM and SAED images of pure and 5% sulfated catalysts are shown in (Figure 7) (a-d). TEM image of Cu(I)@ZrO_2-SO_4^{2-} clearly indicated mesostructured catalyst with nanocrystalline domains. The crystallite size found from TEM micrographs were in good agreement with that calculated by Scherrer method using XRD data.

The TEM image of the pure ZrO_2:Cu(I) material clearly shows core shell structure. Further, the TEM image of Cu(I)@ZrO_2-SO_4^{2-} also shows the retention of this core shell structure.

The SAED patterns of Cu(I)@ZrO_2 showed concentric rings, which indicate the presence of small crystallites with defined positions. These fringes are indexed to the lattice planes (111), (200) and (220), the data clearly correlates with that of XRD of cubic phase ZrO_2:Cu(I). Further, Cu(I)@ZrO_2-SO_4^{2-} also showed clear concentric rings which are indexed to (101), (112) and (211) planes indicating tetragonal phase. The presence of (101) plane was also visualized in HRTEM image Figure 7c. The data obtained is consistent with the literature reported.[45–47]

BET Surface Area Analysis

Variation of surface area of Cu(I)@ZrO_2-SO_4^{2-} catalyst with changes in sulfate loading was evaluated by Brunauer–Emmett–Teller (BET) method. To evaluate the porosity and pore size distribution of the catalyst, Barrett–Joyner–Halenda (BJH)

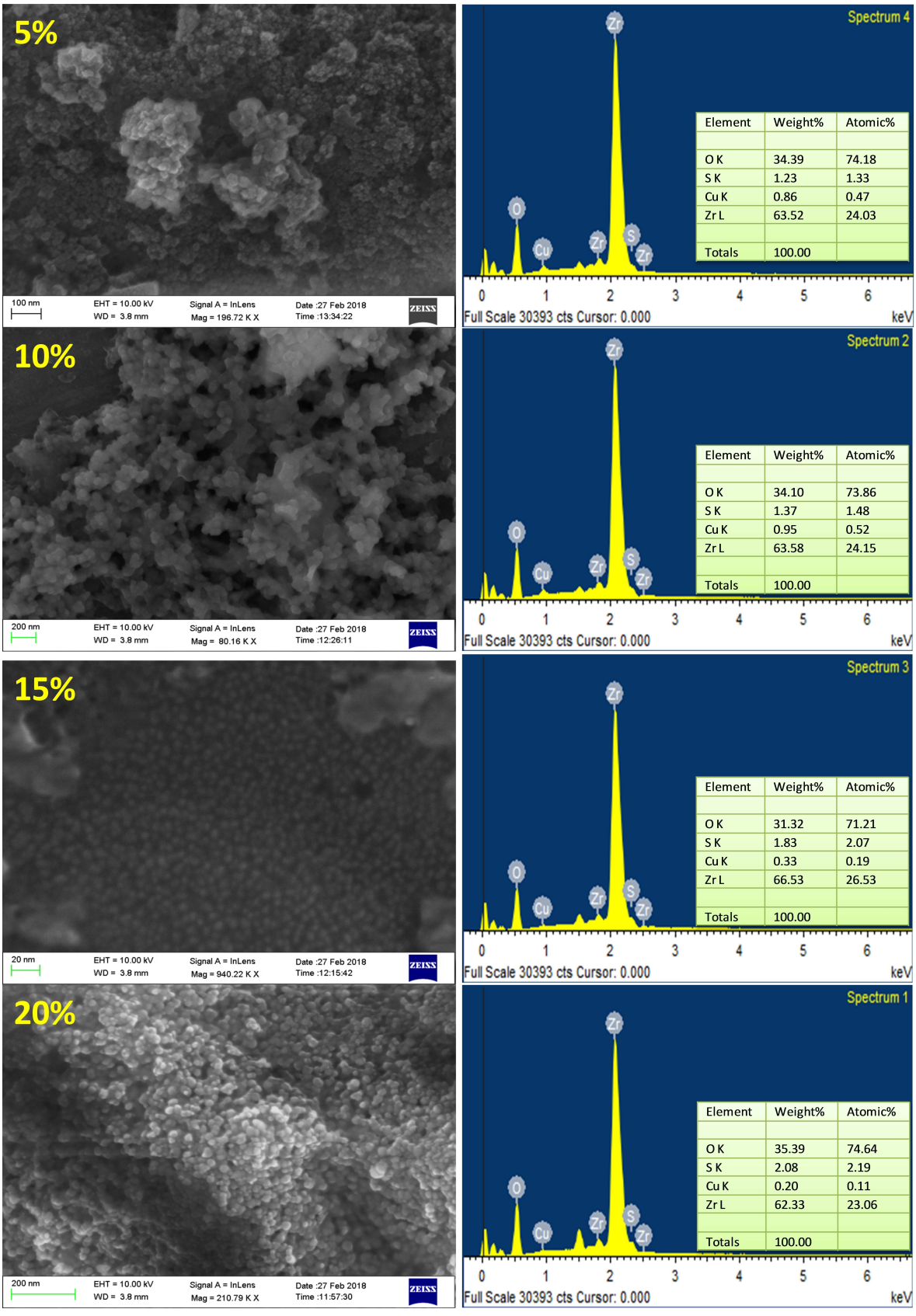

Figure 6. FESEM and EDX images of Cu(I)@ZrO_2-SO_4^{2-} (5-20%)

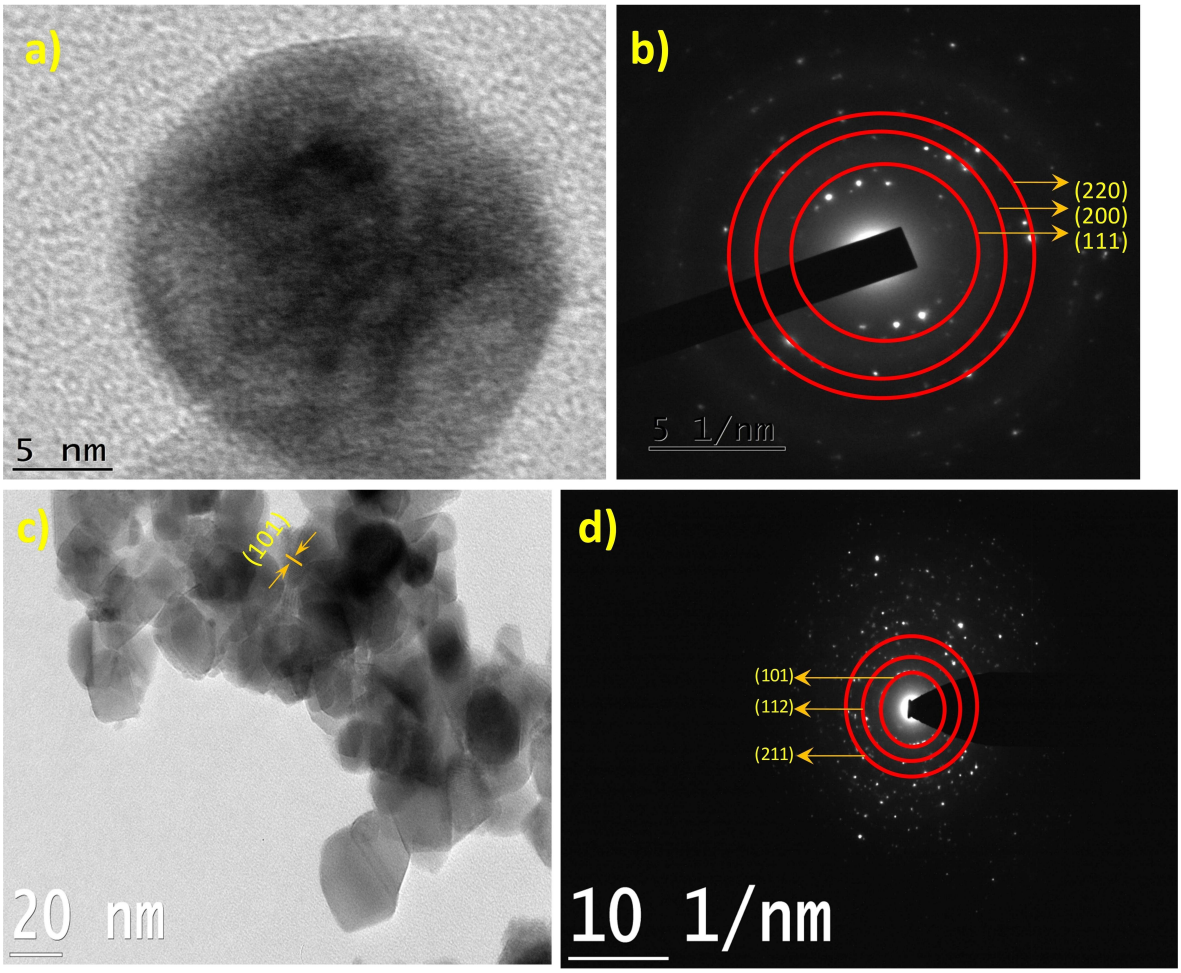

Figure 7. a) and b)TEM and SAED pattern of ZrO_2-Cu(I). c) and d) TEM and SAED pattern of Cu(I)@ZrO_2-SO_4^{2-}

method was used. The N_2 adsorption and desorption plots were shown in the (Figure 8), the data obtained was presented in Table 1.

Table 1. Physico-chemical properties of Cu(I)@ZrO_2-SO_4^{2-} (5-20%)

Percentage sulfate loading	Surface Area (m^2/g)	Pore Volume (cm^3/g)	average pore width (nm)	average pore diameter (nm)
5	59.36	0.3986	26.48	23.34
10	66.04	0.333	19.0	17.09
15	39.31	0.2268	21.6	22.83
20	36.19	0.2075	22.09	17.56

It is clearly evident from the data that, as sulfate ions are introduced to the Cu(I)@ZrO_2 catalyst, the surface area of the catalyst significantly reduced. This is due blockage of surface area by surface occupied sulfate ions.[48,49]

Initially the azo synthesis was performed using pure zirconia and ZrO_2-Cu(I) catalyst. However no sign of diazotization coupling was observed even after a period of 1 hour grinding. However, with Cu(I)@ZrO_2-SO_4^{2-} diazotization coupling was clearly observed, with this success of using solid acid catalyst, optimization studies were performed. Initially effect of amount of catalyst was evaluated, catalytic activity increased with increase in amount of catalyst from 0.05 g to 0.1 g. However, further increase in the amount of catalyst didn't influence on the yield of the azo dye, the optimization data is presented in Table 2.

Further keeping the amount of catalyst to be 0.1 g, the stability of catalyst-diazonium complex was studied. In the typical procedure, the catalyst-diazonium complex formed was stored in dark under desiccation. Coupling was carried out after 24 hours, 5 days, 10 days and 20 days. From the experiments it is evident that, catalyst-diazonium complex showed good stability over the period of. Stability studies of the catalyst-diazonium complex and recycling studies of the catalyst were presented in Table 3.

The catalyst showed good retention of activity even after four cycles. The derivatives of the azo synthesis were listed in Table 4. To reuse the catalyst, it was washed 3 times with ethyl alcohol followed by acetone. Further heated in an hot air oven maintained at 120 °C to reactivate the catalyst. Catalytic

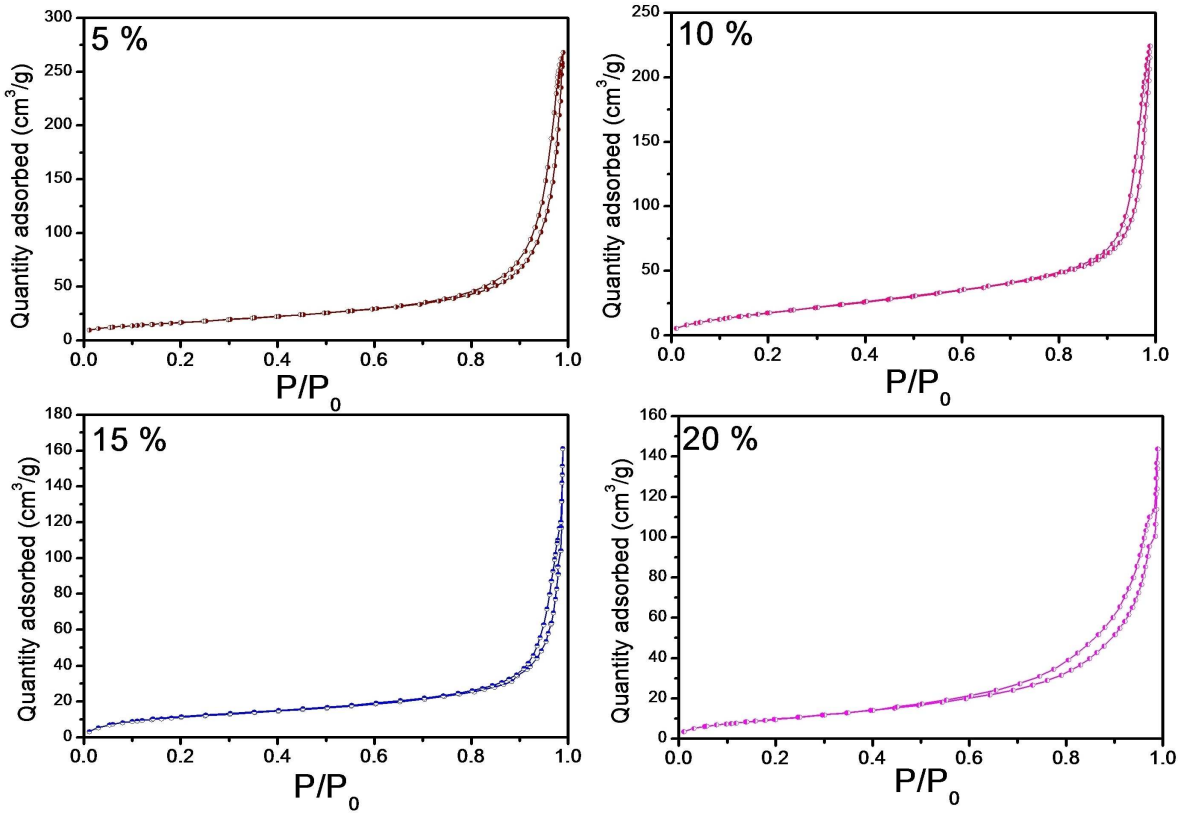

Figure 8. N_2 adsorption-desorption isotherms

Table 2. Optimization studies of catalytic synthesis of azo dyes

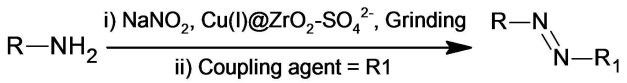

Entry	Catalyst (mg)	Time (h)	Yield* (%)
1	ZrO_2 (Time after grinding)	1 h	-[b]
2	ZrO_2-Cu(I) (Time after grinding)	1 h	-[b]
3	0.1 g Cu(I)@ZrO_2-SO_4^{2-} (5%)	15 min	98
4	0.1 g Cu(I)@ZrO_2-SO_4^{2-} (10%)	15 min	83
5	0.1 g Cu(I)@ZrO_2-SO_4^{2-} (15%)	15 min	78
6	0.1 g Cu(I)@ZrO_2-SO_4^{2-} (20%)	15 min	76
7	0.05 g Cu(I)@ZrO_2-SO_4^{2-} (5%)	15 min	92
8	0.10 g Cu(I)@ZrO_2-SO_4^{2-} (5%)	15 min	98
9	0.15 g Cu(I)@ZrO_2-SO_4^{2-} (5%)	15 min	97
10	0.20 g Cu(I)@ZrO_2-SO_4^{2-} (5%)	15 min	98

*Yield of the product refers to isolated yield

Table 3. Stability of diazonium complex and Recycling studies of Cu(I) @ZrO_2-SO_4^{2-} (5%) catalyst

Entry	Time for coupling	Cycle	Yield*
1	24 h	1	96
2	5 days	1	89
3	10 days	1	83
4	20 days	1	78
5	15 min	1	98
6	15 min	2	95
7	15 min	3	89
8	15 min	4	86

*Yield of the product refers to isolated yield

efficiency was checked for four cycles, which showed marginal loss in the activity.

Conclusions

In the present work a robust Cu(I)@ZrO_2-SO_4^{2-} catalyst was prepared by simple co-precipitation method followed by sulfation using sulfuric acid as a source of sulfate. The prepared material was characterized by XRD, FTIR, Pyridine FTIR, TGA, NH_3-TPD, SEM-EDX, TEM-SAED and BET surface analysis. The catalytic efficiency was evaluated against the synthesis of azo dyes from substituted aniline and other coupling agents. Catalyst exhibited cubic phase initially and on sulfation it changed to tetragonal phase. This tetragonal phase was stable and retained by the catalyst even at high sulfate loading. Decrease in acidic strength was observed with increase in sulfate loading as evident from the NH_3-TPD data. Presence of both Bronsted and Lewis acid sites are confirmed by both pyridine-FTIR and NH_3-TPD. Incorporation of sulfate ions and its subsequent effect on the morphology of the catalyst was shown in FESEM micrographs, this is further confirmed by TEM analysis. Crystal phases were ascertained by concentric rings of SAED pattern, which correlates well with the XRD data. BET

Table 4. Synthesis of azo dyes using various amines and aromatic coupling agents

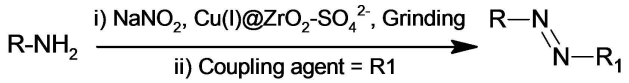

Where R = Substituted benzene ring
R1 = 1-napthol, 2-napthol, 2-chloro phenol, phenol and salicylaldehyde

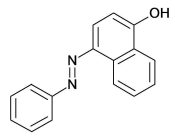
3a. 90%

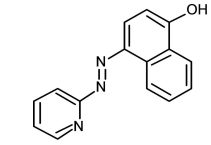
3b. 94%

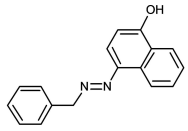
3c. 87%

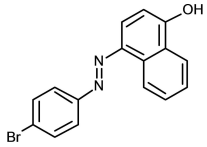
3d. 92%

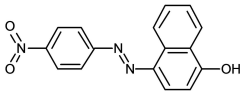
3e. 96%

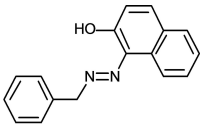
3f. 89%

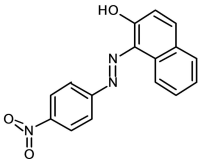
3g. 98%

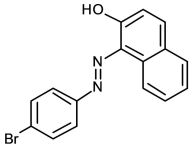
3h. 93%

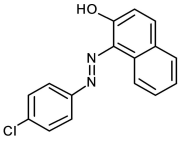
3i. 93%

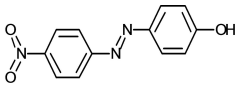
3j. 95%

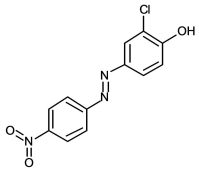
3k. 93%

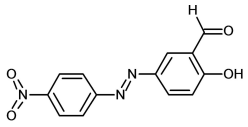
3l. 92%

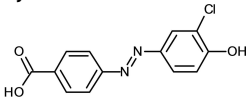
3m. 83%

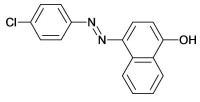
3n. 86%

surface analysis indicates decrease in surface area with increase in the sulfate loading. Among the four sulfate loaded catalyst, 5% sulfate loaded Cu(I)@ZrO_2-SO_4^{2-} catalyst showed significantly better catalytic activity, which could be attributed to high acidity arising due to high Bronsted and Lewis sites. A good comparison of catalytic activity with B/L acidity ratio was observed. Reuse of catalyst showed marginal loss in the performance even after four cycles, which shows Cu(I)@ZrO_2-SO_4^{2-} is proven to be a good solid acid catalyst for the synthesis of azo dyes under environmentally benign process.

Suppoting Information Summary

Materials and experimental methods with general method for the preparation of catalyst and azo dyes are provided in the supporting information. ^{1}H NMR and ^{13}C NMR spectra of the compounds and their interpretation are provided in the supporting information.

Acknowledgements

The Authors S.S. and L. P are grateful to Sophisticated Instrumentation facility, School of Advanced Sciences, Chemistry division, VIT University, Vellore, NMR Center IISc, Bangalore, for the technical support in spectral data curation. The authors are grateful to TEQIP II and DST Nano Mission, Siddaganga Institute of Technology, Tumkur and SIF Karnataka University, Dharwad. for the support rendered in successful completion of this research work.

Conflict of Interest

The authors declare no conflict of interest.

Keywords: Azo dyes · Core-shell Cu(I)@ZrO_2-SO_4^{2-} · Green chemistry · Solvent free. Sulfated Solid acid catalyst

[1] M. Mariani, F. Zaccheria, N. Scotti, R. Psaro, N. Ravasio, *Chem. Sel.* **2016**, *1*, 2999–3004.
[2] Y. C. S. and B. Singh, *Biofuels, Bioprod. Biorefining* **2011**, *5*, 69–92.
[3] J. H. Clark, *Acc. Chem. Res.* **2002**, *35*, 791–797.
[4] M. S. Tiwari, A. B. Gawade, G. D. Yadav, *Green Chem.* **2017**, *19*, 963–976.
[5] P. Bhaumik, P. L. Dhepe, *Catal. Rev.* **2016**, *58*, 36–112.
[6] M. Breugst, K. N. Houk, *J. Org. Chem.* **2013**, *78*, 9892–9897.
[7] S. De, S. Dutta, B. Saha, *Catal. Sci. Technol.* **2016**, *6*, 7364–7385.
[8] M. T. Lanagan, J. K. Yamamoto, a. Bhalla, S. G. Sankar, *Mater. Lett.* **1989**, *7*, 437–440.
[9] F. Shojai, T. A. Mäntylä, *J. Eur. Ceram. Soc.* **2001**, *21*, 37–44.
[10] Y. Kong, H. X. Ma, J. Wang, X. Q. Ren, Q. J. Yan, *Chinese J. Chem.* **2005**, *23*, 1584–1588.
[11] E. M. Albuquerque, L. E. P. Borges, M. A. Fraga, C. Sievers, *ChemCatChem* **2017**, *9*, 2675–2683.
[12] M. L. Grecea, A. C. Dimian, S. Tanase, V. Subbiah, G. Rothenberg, *Catal. Sci. Technol.* **2012**, *2*, 1500–1506.
[13] G. K. Chuah, S. Jaenicke, B. K. Pong, *J. Catal.* **1998**, *175*, 80–92.
[14] N. Katada, J. I. Endo, K. I. Notsu, N. Yasunobu, N. Naito, M. Niwa, *J. Phys. Chem. B* **2000**, *104*, 10321–10328.
[15] V. T. Vasantha, N. J. Venkatesha, Z. M. Shamshuddin, J. Q. D'Souza, B. G. V. Reddy, *Chem. Sel.* **2018**, *3*, 602–608.
[16] G. D. Yadav; M. S.Krishnan, *Recent Adv. Basic Appl. Asp. Ind. Catal. Stud. Surf. Sci. Catal.* **1998**, *113*, 259–265.
[17] R. S. Drago, N. Kob, *J. Phys. Chem. B* **1997**, *101*, 3360–3364.
[18] J. Liu, J. Zhao, C. Miao, Y. Yue, W. Hua, Z. Gao, *Chinese J. Chem.* **2011**, *29*, 1095–1100.
[19] L. Parashuram, S. Sreenivasa, S. Akshatha, V. U. Kumar, S. Kumar, *Asian J. Org. Chem.* **2017**, *6*, 1755–1759.
[20] P. K. Khatri, N. Karanwal, S. Kaul, S. L. Jain, *Tetrahedron Lett.* **2015**, *56*, 1203–1206.
[21] G. Kuriakose, N. Nagaraju, *J. Mol. Catal. A Chem.* **2004**, *223*, 155–159.
[22] T. Vijai Kumar Reddy, G. Sandhya Rani, R. B. N. Prasad, B. L. A. Prabhavathi Devi, *RSC Adv.* **2015**, *5*, 40997–41005.
[23] Q. Xia, C. Li, Y. Zhang, C. Qi, F. Zhang, *Chem. Sel.* **2018**, *3*, 9232–9235.
[24] L. Muraleedharan, B. M. Chandrashekara, B. S. J. Prakash, Yajnavalkya, S. Bhat, *Chem. Sel.* **2018**, *3*, 801–808.
[25] P. Ncube, R. W. Krause, B. B. Mamba, *Sensors* **2011**, *11*, 4598–4608.
[26] S. B. Patil, B. Kishore, M. K. Nagaraj, N. Ganganagappa, U. Velu, *Chem. Sel.* **2018**, *3*, 7490–7495.
[27] A. R. Yuvaraj, G. S. Mei, A. D. Kulkarni, M. Y. Mashitah, G. Hegde, *RSC Adv.* **2014**, *4*, 50811–50818.
[28] V. Chigrinov, H. S. Kwok, H. Takada, H. Takatsu, *Liq. Cryst. Today* **2005**, *14*, 1–15.
[29] M. I. Uddin, S. M. Evans, J. R. Craft, L. J. Marnett, M. J. Uddin, A. Jayagopal, *ACS Med. Chem. Lett.* **2015**, *6*, 445–449.
[30] J. F. Morin, *J. Mater. Chem. C* **2017**, *5*, 12298–12307.
[31] M. Watanabe, *Sci. Technol. Adv. Mater.* **2017**, *18*, 705–723.
[32] G. Hallas, J.-H. Choi, *Dyes. Pigm.* **1999**, *40*, 119–129.
[33] J. Qiu, B. Tang, B. Ju, Y. Xu, S. Zhang, *Dyes. Pigm.* **2017**, *136*, 63–69.
[34] H. Valizadeh, A. Shomali, S. Nourshargh, R. Mohammad-Rezaei, *Dyes. Pigm.* **2015**, *113*, 522–528.
[35] A. N. Chermahini, M. Doukheh, H. Z. Hassan, M. Bostanian, *J. Ind. Eng. Chem.* **2012**, *18*, 826–833.
[36] A. Zarei, A. R. Hajipour, L. Khazdooz, B. F. Mirjalili, A. Najafi, *Dyes. Pigm.* **2009**, *81*, 240–244.
[37] A. D'Epifanio, M. A. Navarra, F. Christoph Weise, B. Mecheri, J. Farrington, S. Licoccia, S. Greenbaum, *Chem. Mater.* **2010**, *22*, 813–821.
[38] K. J. A. Raj, M. G. Prakash, R. Shanmugam, K. R. Krishnamurthy, B. Viswanathan, *Indian J. Chem.* **2011**, *50*, 1050–1055.
[39] P. Manjunathan, V. S. Marakatti, P. Chandra, A. B. Kulal, S. B. Umbarkar, R. Ravishankar, G. V. Shanbhag, *Catal. Today* **2018**, *309*, 61–76.
[40] M. A. Bhosale, T. Sasaki, B. M. Bhanage, *Catal. Sci. Technol.* **2014**, *4*, 4274–4280.
[41] E. Rubio, V. Rodriguez-lugo, R. Rodriguez, *Nano* **2009**, *22*, 67–73.
[42] R. Srinivasan, R. A. Keogh, D. R. Milburn, B. H. Davis, *J. Catal.* **1995**, *153*, 123–130.
[43] P. Manjunathan, R. Ravishankar, G. V. Shanbhag, *ChemCatChem* **2016**, *8*, 631–639.
[44] C. Huang, A. Li, Z. S. Chao, *RSC Adv.* **2017**, *7*, 48275–48285.
[45] T. Tätte, M. Part, R. Talviste, K. Hanschmidt, K. Utt, U. Mäeorg, I. Jõgi, V. Kiisk, H. Mändar, G. Nurk, *RSC Adv.* **2014**, *4*, 17413–17419.
[46] G. Katz, *J. Am. Ceram. Soc.* **1971**, *54*, 531.
[47] P. Duwez, F. Odell, *J. Am. Ceram. Soc.* **1947**, *30*, 274–283.
[48] A. Rachmat, W. Trisunaryanti, Sutarno, K. Wijaya, *Mater. Renew. Sustain. Energy* **2017**, *6*, 1–9.
[49] F. R. Chen, G. Coudurier, J. F. Joly, J. C. Vedrine, *J. Catal.* **1993**, *143*, 616–626.

Submitted: October 21, 2018
Accepted: March 27, 2019